

RELATIVISTIC HEAVY-ION EXPERIMENTS

Howel G. Pugh

Nuclear Science Division
Lawrence Berkeley Laboratory
University of California
Berkeley, CA 94720, U.S.A.

Invited paper presented at the XII International
Symposium on Multiparticle Dynamics, Notre Dame,
June 21-26, 1981

This work was supported by the Director, Office of Energy
Research, Division of Nuclear Physics of the Office of High Energy
and Nuclear Physics of the U.S. Department of Energy under Contract
W-7405-ENG-48.

RELATIVISTIC HEAVY ION EXPERIMENTS

Howel G. Pugh
Nuclear Science Division
Lawrence Berkeley Laboratory
University of California
Berkeley, CA 94720, U.S.A.

ABSTRACT

Objectives of high energy nucleus-nucleus studies are outlined. Bevalac experiments on the formation of hot high-density equilibrated nuclear matter are discussed. Future programs are outlined, including research at the CERN ISR.

INTRODUCTION: DENSITIES AND TEMPERATURES

In this paper I will give a summary of the principal objectives for studies of high energy nucleus-nucleus collisions. I will describe some experiments done at the Bevalac with emphasis on aspects of most interest to higher energy studies, namely, whether an equilibrium state is produced and how its properties can be diagnosed. Finally, I will discuss the next stages of experiment and the extension to very high energies to study quark-gluon plasmas, with the σ - α experiments at the ISR as an important milestone along the way. References 1-5 provide extensive material for further study.

1. Objectives

The primary objective for the study of very high energy nucleus-nucleus collisions is to observe the properties of nuclear matter under conditions of high density and temperature. Our understanding of astrophysics requires a knowledge of the equation of state of nuclear matter at densities ranging from a fraction of normal to many times normal. Significant phase changes of nuclear matter are suspected to occur in neutron stars; transitions to quark or hadronic phases are possible at the centers of very dense stars. Our understanding of cosmogenesis likewise requires a knowledge of this subject: in the first seconds, if the "big bang" theory is correct, the universe expanded and cooled rapidly through a quark-gluon phase into a hot, high-density nuclear matter phase. However, we do not know enough about the hadronic interaction to predict the behavior of nuclear matter as the density is increased or to predict much about the quark-gluon phase except its existence. Experiment is therefore essential and high energy collisions between heavy nuclei seem to be the only avenue. The results of such studies may not only give us the empirical information required for astrophysical and cosmological studies but may also cast light on the hadronic interaction, especially on the origin of confinement. If we can understand how nuclear matter behaves when the nucleons merge into each other producing the quark-gluon phase, we will understand the confinement mechanism.

2. Phase Diagram and Equilibrium Paths

Figure 1 shows a phase diagram for nuclear matter with some predictions of transitions from normal nuclear matter to hadronic

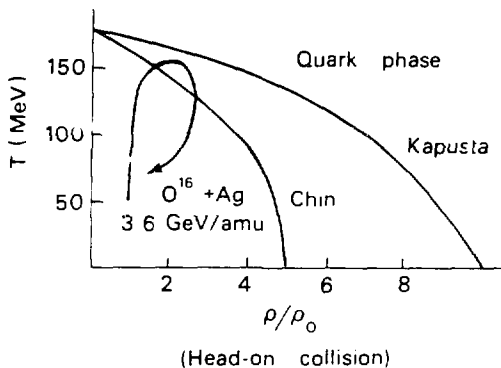


Fig. 1. Phase diagram for nuclear matter and trajectory followed during a heavy ion collision.

and quark phases. The presentation of such a diagram presupposes an equilibrium condition at each point, such as can be maintained in stars under the influence of "external", i.e., gravitational, forces. The region of the diagram that is accessible to low energy nuclear physics is confined to a small region near normal density. If, as in stars, we could increase the pressure while keeping the temperature low, we might find interesting new bound states such as pion condensates or density isomers as we proceed towards the quark-gluon phase. Increasing the temperature at constant density would also lead us to the quark-gluon phase, but we would be exploring a different aspect of its properties.

Heavy ion collisions produce at best a series of quasi-equilibrium states. The reaction path indicated by the arrow in Figure 1 is typical of a collision at Bevalac (or Synchrotron) energies. It was obtained from an intranuclear cascade calculation⁶ using nucleon-nucleon data as input. The calculation shows that the transition to quark-gluon matter is approached even at these low energies. Such calculations are reliable as long as we do not stray too far from ordinary nuclear matter conditions. They provide a very useful basis of expectation with which to confront observations and provide information on a variety of features. They tell us that the high density period of the collision lasts only 10^{-23} or 10^{-22} seconds. We therefore have to disentangle the equation of state from the reaction dynamics, which are only to a limited extent under our control. However, there are many properties we can measure. For example, Figure 2 shows the prediction of another cascade calculation⁷ how the composition of the nucleus must change as the density is increased by increasing the bombarding energy. At 1 GeV/amu, 20% of the nucleons should be converted to isobars.

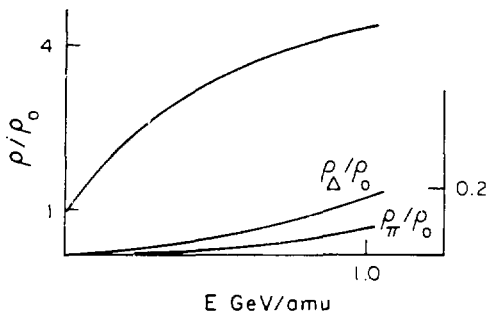


Fig. 2. Changing composition of nuclear matter with increasing density (achieved by increasing bombarding energy).

3. Temperatures from Pion Spectra

Experiments with high energy heavy ions have so far been carried out only at the Bevalac (2.1 GeV/amu, ions up to Fe) and the Synchrophasotron (4 GeV/amu, ions up to Ne). High temperatures are indeed reached in these experiments. Figure 3 shows π^-

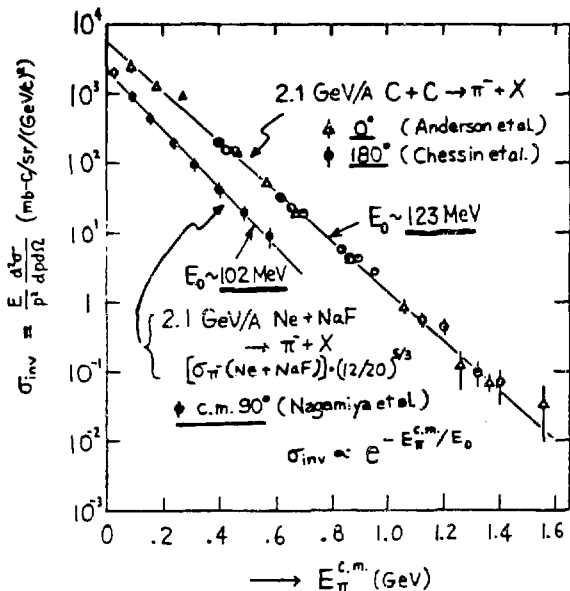


Fig. 3. Pion inclusive spectra measured in heavy ion collisions. Data from reference 8.

energy spectra from C + C collisions and Ne + NaF collisions at 2.1 GeV/amu.⁸ (NaF is used to simulate a Ne target for the study of equal mass collisions.) The spectra are seen to be exponential--this seems to be true at all angles and all energies; if the inverse slope is interpreted in terms of a temperature, the temperature is very high. The slope does not vary greatly with angle--for C + C at 0° it is (123 MeV)⁻¹ while for Ne + NaF at 90° it is (102 MeV)⁻¹.

If we plot the inverse slope (temperature) against bombarding energy, we find the systematic dependence shown in Figure 4.⁹

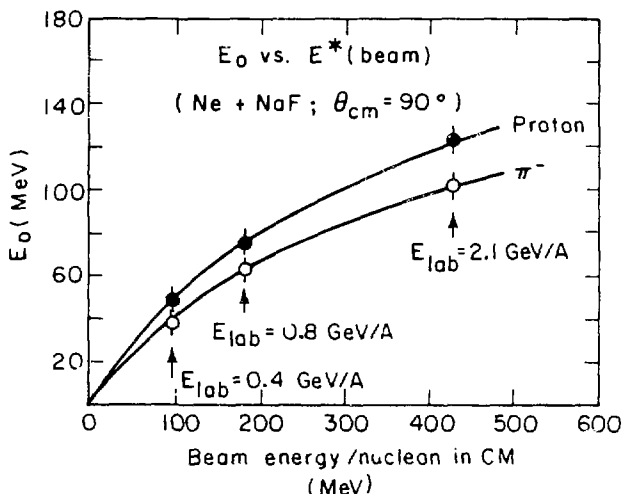


Fig. 4. Energy dependence of the "temperature" E_0 in Ne + NaF collisions. Data from reference 9.

For this, only data at 90° c.m. have been used because these may be the least dependent on assumptions made about the reaction mechanism. The temperatures observed reflect the final state of the colliding system and initial temperatures may be higher. We have little proof of the densities reached except insofar as the calculations that predict them seem to be in general accord with other observations. It should also be remarked that the inclusive spectra from which these temperatures are deduced reflect an average over impact parameters. Conditions for selected impact parameters are of greater interest, as will be discussed below.

Before turning from inclusive pion spectra to central collisions, it is of interest to show Figure 5. This presents data on pion production⁸ at the laboratory energy of 200 MeV/amu (only

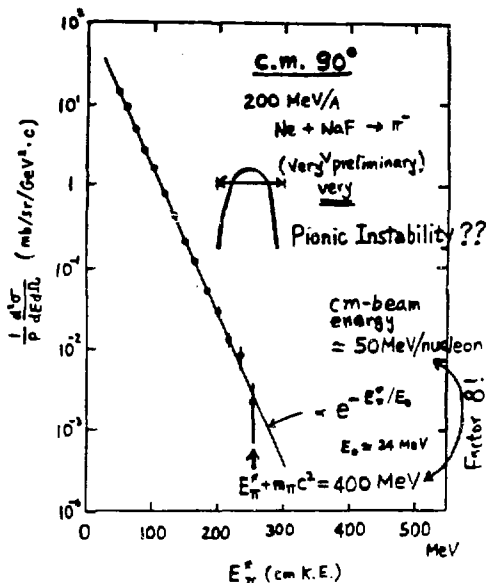


Fig. 5. Pion production at 90° with 200 MeV/amu beams. Preliminary data from ref. 8. No evidence for a pionic instability is found.

50 MeV/amu in the c.m. system). The microbarn cross sections are among the lowest so far measured at the Bevalac. This measurement was made to test a prediction¹⁰ that a break in the slope of the invariant cross section would signal transient radiation associated with the onset of formation of a pion condensate. At this bombarding energy, no effect is seen as big as 1% of the prediction.

CENTRAL COLLISIONS

The question of whether and under what conditions equilibrium systems can be produced in heavy ion collisions is of capital importance to the whole field of research, and many studies are focused on this question. Most calculations predict that the optimum conditions for producing and studying high density states would be in head-on or "central" collisions.

1. Selection of Central Collisions and Pion Production

Central collisions are usually selected by means of a type of trigger developed by the Riverside streamer-chamber group. The principle is that in a grazing collision many nucleons in the projectile will not interact and will proceed in the forward direction ("target fragmentation"). At the highest energy of the Bevalac these fragments fall in a forward cone of half angle about 6° . Their momentum distribution seems to be consistent with the

Fermi distribution in the projectile nucleus combined with the beam velocity. The central trigger selects events in which few or no fragments of the projectile appear in the forward direction.

Figure 6 shows the schematic layout for such a trigger. The detectors respond to Z_i^2 where Z_i is the charge of each particle. Since Z_1^2 is greatest when all the charge is concentrated on one particle, the upstream detector has the maximum pulse height (corresponding to the beam particle) and the downstream detector has a continuous distribution of pulse height down to zero. Cascade calculations¹¹ indicate that for equal mass target and projectile this should give a unique measure of impact parameter. For unequal masses additional information would be necessary.

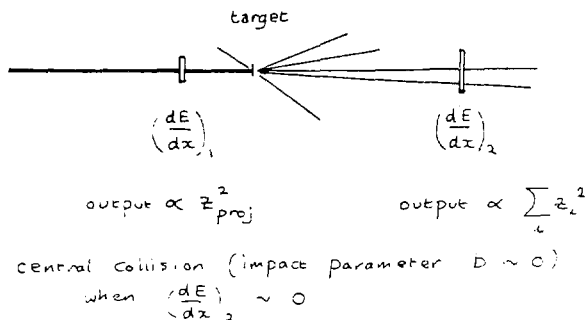


Fig. 6. Schematic diagram of the central trigger.

Figure 7 shows the effect of such a trigger selection on streamer chamber data¹² for $^{40}\text{Ar} + \text{KCl}$ collisions at 1.8 GeV/amu. The total number of charged particles per collision n_{ch} and the number of negative pions n_{π^-} are shown for unbiased selection of inelastic interactions (solid points) and for central collisions selected by the trigger (open points). The trigger selects 10% of the total inelastic cross section and corresponds to impact parameters less than about 2.4 fm. The effect of the trigger on both n_{ch} and n_{π^-} is striking.

The particle multiplicities shown in Fig. 7 extend up to very high values. The average number of charged particles in a central collision is $\langle n_{ch} \rangle \sim 42$, and the average number of pions is $\langle n_{\pi^-} \rangle = 3 \langle n_{\pi^+} \rangle \sim 18$. It is clear that in a substantial fraction of events both nuclei must be completely disintegrated. The general picture is one of about 100 secondary particles (including neutrons) including about 20 pions.

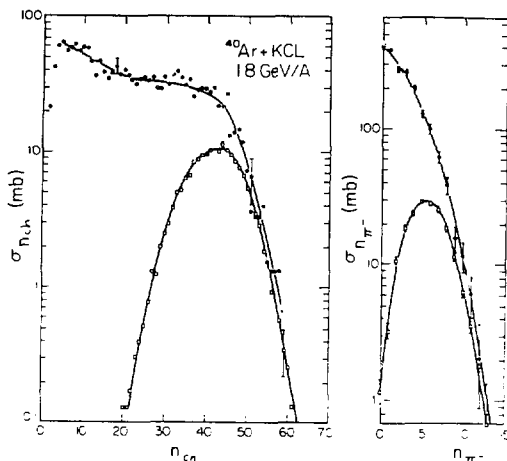


Fig. 7. Total charged particle n_{ch} and negative pion n_{π^-} multiplicity distributions taken with (lower curves) and without (upper curves) a central trigger bias. Data from reference 12.

The energy dependence of the π^- multiplicity is shown in Figure 8. This excitation function tests early predictions that a

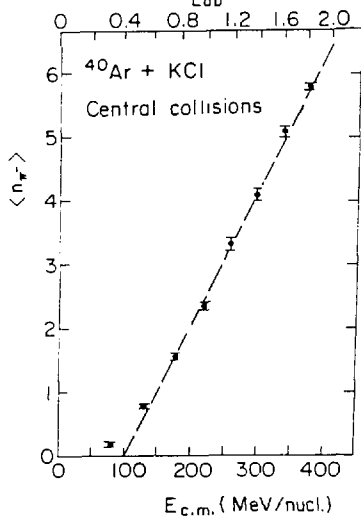


Fig. 8. Energy dependence of multiplicity in central $^{40}\text{Ar} + \text{KCl}$ collisions. Data from reference 12.

signature for pion condensation would be a step in the pion multiplicity as a function of beam energy. There is no such step at a level of more than a few per cent in the Bevalac energy range.

Isotropy of the particle emission and energy spectra is not necessary for thermodynamical descriptions to be useful. For a detailed discussion of this see Hagedorn¹³. However, it is interesting to explore to what extent a global equilibrium is reached in central collisions and to try to deduce the geometric shape of the interaction region.

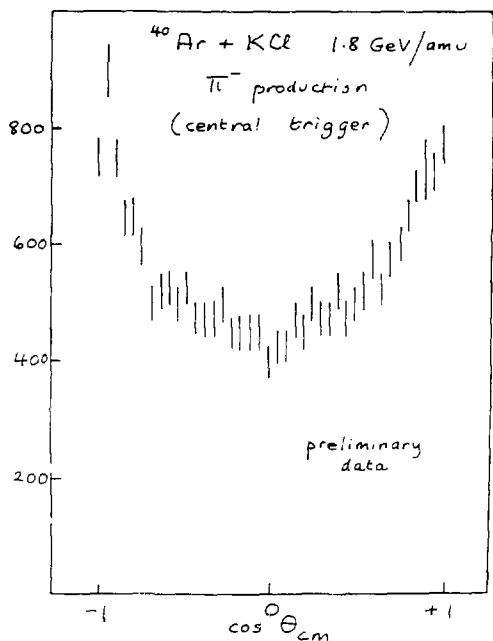


Fig. 9. Angular distribution of pions produced in central $^{40}\text{Ar} + \text{KCl}$ collisions at 1.8 GeV/amu. Preliminary data from reference 14.

Figure 9 shows the angular distribution of π^- for central collisions¹⁴. It is forward-backward peaked but not markedly so. The energy spectra for central collisions are still being analyzed. It will be interesting to compare them with the inclusive data.

2. Intensity Interferometry

Intensity interferometry has become a much-used method for studying the source properties when multiple particle emission is probable¹⁵. Heavy ion collisions provide a new opportunity to use this technique. Basically, pairs of identical particles are observed (in this case negative pions) and the correlation function

$$C_2(\vec{p}_1, \vec{p}_2) = \frac{N(\vec{p}_1, \vec{p}_2)}{N(\vec{p}_1)N(\vec{p}_2)}$$

is measured. The choice of $N(\vec{p})$ is somewhat problematical, especially if strong correlations are observed. Assuming that this problem can be taken care of, and assuming that the pions are emitted from a source with gaussian form in both space and time, it can be shown that

$$C(\vec{p}_1, \vec{p}_2) = N \left\{ 1 + a \exp \left[-\frac{1}{2} |\vec{p}_1 + \vec{p}_2|^2 R^2 \exp -\frac{1}{2} (E_1 - E_2)^2 T^2 \right] \right\}$$

The quantities R and T represent the spatial and temporal extent of the source. The quantity a reflects the degree of incoherence of the source and should be between 0 and 1.

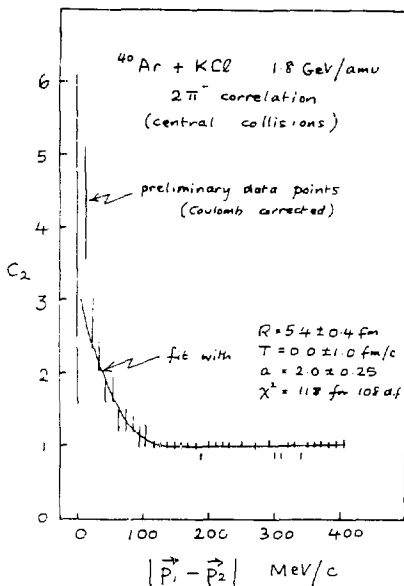


Fig. 10. Intensity interferometry of negative pions from central $^{40}\text{Ar} + \text{KCl}$ collisions at 1.3 GeV/amu. Preliminary streamer chamber data from reference 14.

In our experiments¹⁴ the data were taken from the streamer chamber measurements. They were corrected for the small Coulomb repulsion between the pions. $N(\vec{p}_1, \vec{p}_2)$ was extracted using all possible pairs of pions and the background was calculated taking pairs of pions from different events of the same multiplicity.

Figure 10 shows preliminary results for the correlation and the extracted source parameters. The time parameter T is found to be zero with a large uncertainty. The source radius $R = 5.4 \pm 0.4$ fm, rather larger than the nuclear radius of about 4 fm.

The correlation parameter a seems to lie outside the range of values permitted by the simple theory. The preliminary value of 2.0 ± 0.25 is larger than any previously observed in such systems as $\pi\pi$, pp , etc., where it rarely approaches the value of unity. Recent theoretical work by Gyulassy¹⁶ has shown that once the simple assumptions made about the source are relaxed, the parameter a may take on a wide range of values. Clearly this is a hot topic to pursue.

Even though it is not strictly valid, we have tried to separate out parts of the data that might reflect a nonspherical shape for the interaction region. We divided the data into forward, backward, and side cones of half angle 45° as shown in Figure 11. The extracted values for R , T , and a are also shown in the figure. The analysis suggests a nonisotropic source, but a more elaborate analysis should be performed, especially if the assumption of incoherence has to be abandoned as implied by the large value of the parameter a .

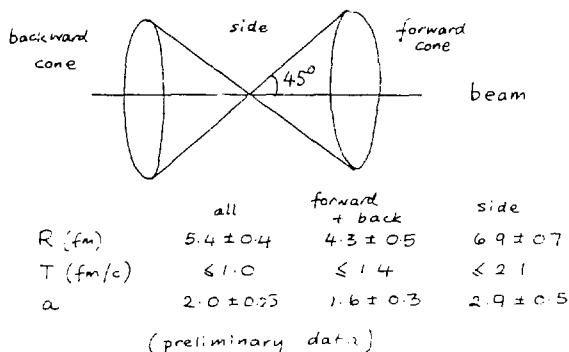


Fig. 11. Effect of selecting longitudinally or transversely emitted pion pairs on the parameters extracted by intensity interferometry. Preliminary data from reference 14.

3. Cluster Analyses

In order to extract dynamic information from cluster analyses, completely reconstructed events are desirable. So far, we have only a few dozen fully measured streamer chamber events, and these do not yet have particle identification. However, we have many events in which all the π^- have been measured, so it seemed interesting to try out the various methods on the negative pions by themselves. We have made thrust, sphericity, and minimal spanning tree analyses of these data. As an illustration a sphericity distribution is shown in Figure 12. This result appears interesting until we

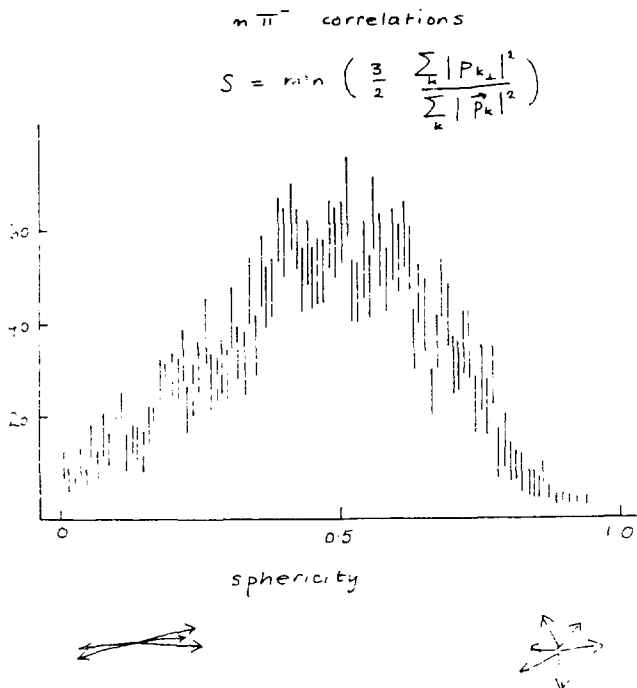


Fig. 12. Sphericity analysis of negative pion distributions produced in $^{40}\text{Ar} + \text{KCl}$ central collisions at 1.8 GeV/amu. Preliminary data from reference 14.

compare with Figure 13 where the same results are shown divided by an artificial set generated by creating events of the same multiplicity by taking each pion from a different event, also of the same multiplicity. It is thus seen that the sphericity

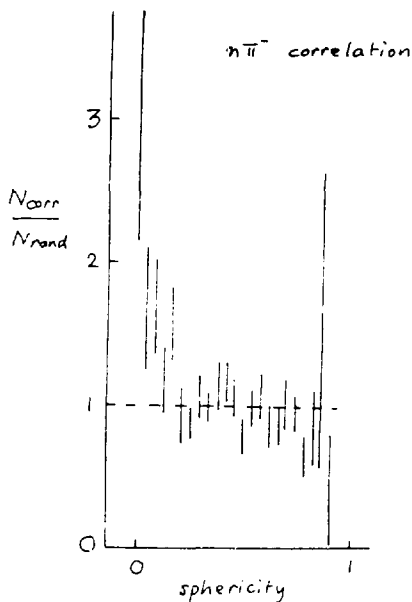


Fig. 13. Ratio between the sphericity distribution of Fig. 12 and a distribution generated by choosing pions from different events. Preliminary data from reference 14.

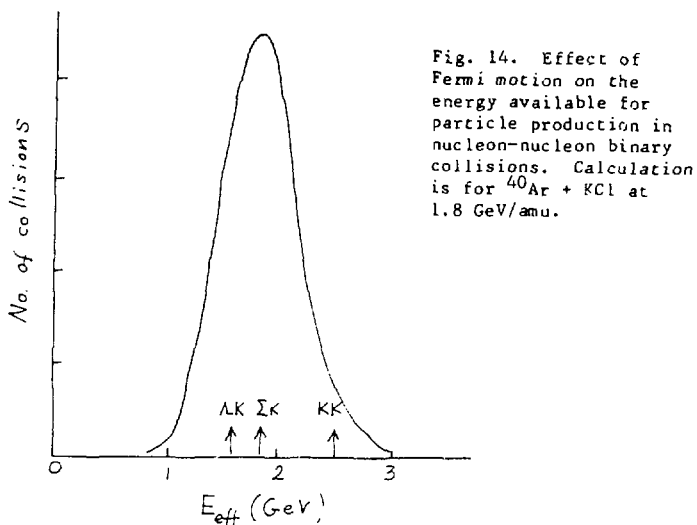
distribution contains no new information beyond what was present in the multiplicity distribution and the pion spectra taken separately.

Such analyses are still in the earliest stages and we have not yet been able to apply them to data expected to contain important dynamic information.

4. Strange Particle Production

The Bevalac is close to the production threshold for K , Λ , Σ in nucleon-nucleon collisions. Figure 14 shows the thresholds and the effective nucleon-nucleon energy in $^{40}\text{Ar} + \text{KCl}$ collisions at 1.8 GeV/amu including the Fermi motion in both target and projectile. The majority of the particle pairs are above threshold for associated production but below threshold for pair production of kaons.

The Λ spectra have been measured at the streamer chamber for central collisions of $^{40}\text{Ar} + \text{KCl}$ at 1.8 GeV/amu.¹⁷ The cross section for Λ production is 7.6 ± 2.2 mb for central collisions having a cross section of 180 mb (impact parameter < 2.4 fm). This gives 0.04 Λ per central collision on the average.



About 50 Λ s have been observed as shown in the momentum scatter plot of Figure 15. These data are not corrected for detection efficiency. The shaded area has detection efficiency equal to zero. The circle shows the phase space limit for Λ production in three nucleon-nucleon collisions at the beam energy.

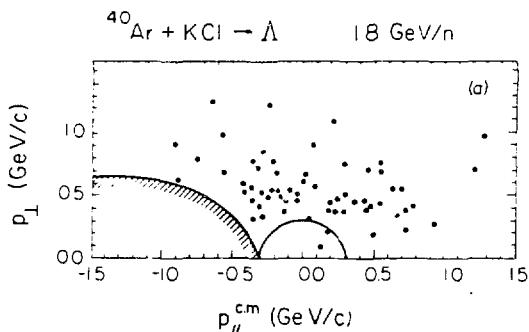


Fig. 15. Scatter plot of Λ production in the streamer chamber, as a function of p_{\parallel} and p_{\perp} (c.m.). Data from reference 17.

Table I shows the mean transverse and longitudinal Λ momenta (efficiency corrected). It is interesting that the average transverse momentum is about the same as the average longitudinal momentum. For an isotropic distribution it would be greater by a factor of $\sqrt{2}$.

Table I

Average transverse and longitudinal momenta in the cm system for Λ production in $^{40}\text{Ar} + \text{KCl}$ at 1.8 GeV/amu, compared with various calculations

	p_{\perp} (GeV/c)	p_{\parallel} (GeV/c)
Data	0.49	0.43
AA	0.21	0.21
RS (fireball)	0.22	0.23
RS (initial)	0.28	0.64

The results of three simple attempts to explain the data are also shown in the table. The AA calculation includes only Fermi motion of the interacting nuclei. It clearly fails to introduce sufficient high momentum components. The RS (fireball) calculation shows the effect of introducing one rescattering of the (approximately the expected number) from an equilibrated system with a temperature determined from the pion spectrum. This also fails. The RS (initial) calculation uses one rescattering from a system in which all the nucleons still have their initial momenta. This boosts the longitudinal momenta by more than the required amount but still does not adequately explain the transverse momenta. The partial success for the third model is consistent with the idea that production occurs in the very first collisions, before the nucleon energies have fallen below the production threshold and a fortiori before an equilibrated system has been produced. However, this model has not explained the transverse momentum distribution. Additional data have been accumulated to study this further.

Since Λ s are self-analyzing for polarization, it was easy to extract a measure of the polarization:

$$P = -0.10 \pm 0.05.$$

This result does not yet have the accuracy to complement high energy p-p data. Again we look to improved statistics using recent streamer chamber exposures.

The above measurements for central collisions are complemented by inclusive K^+ data.⁸ These are shown in Fig. 16 where data from various angles have been combined. Once again it is found that rescattering of the outgoing particle is necessary to explain

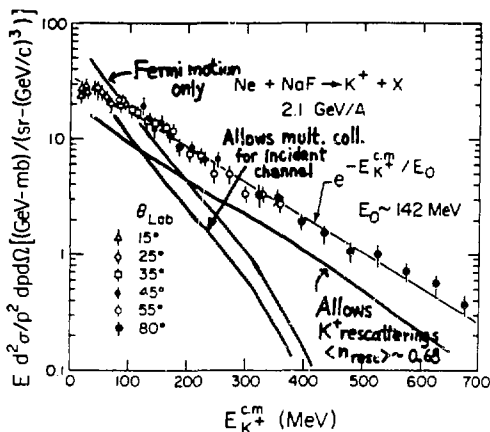


Fig. 16. The K^+ spectrum in 2.1 GeV/amu Ne + NaF collisions. Preliminary data from reference 8.

the shape of the spectrum. Unfortunately the absolute cross section for production in nucleon-nucleon collisions is only known within a factor of two at these energies, so it is not known whether the discrepancy in absolute yield is significant.

Recent unpublished measurements at Berkeley¹⁸ have shown that K^- production also occurs even though the threshold for K^+K^- production (2.5 GeV) is well above the beam energy per nucleon. An interesting possibility is that the K^- is produced by secondary interaction of a Λ or Σ in the hot nuclear system. This would permit some interesting tests of chemical equilibrium and of the constitution of the nuclear system during the collision.

COMPOSITE PARTICLE PRODUCTION

Initial results at the Bevalac supported qualitatively the idea that deuterons and tritons are produced by coalescence of nucleons produced in some primordial fireball. Recent precise data shown some remarkable systematic behavior.⁸

It is found that a power law relation enables d , t , etc., inclusive spectra to be predicted from the proton spectra from the same reaction, i.e.,

$$E_A \frac{d^3 \sigma_A}{d p_A^3} = C_A \left(E_p \frac{d^3 \sigma_p}{d p_p^3} \right)^A$$

where the left-hand side refers to the production of fragments of mass A at momentum p_A and the right-hand side refers to the production of protons of momentum p_p where $p_p = (1/A)p_A$. The quantity C_A is a constant.

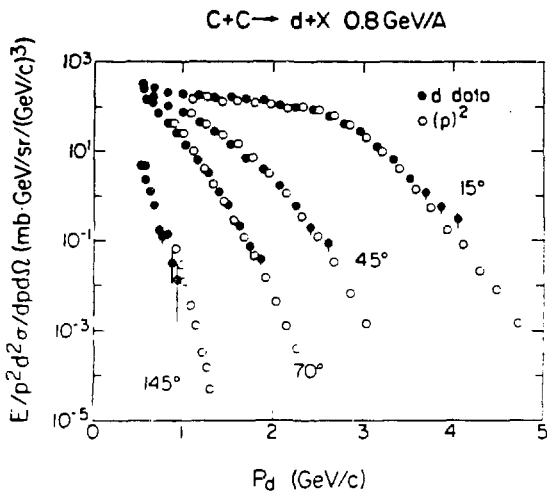


Fig. 17. Deuteron inclusive spectra from heavy ion collisions at 0.8 GeV/amu showing also the square of the proton inclusive spectra at the same angles. Data from reference 9.

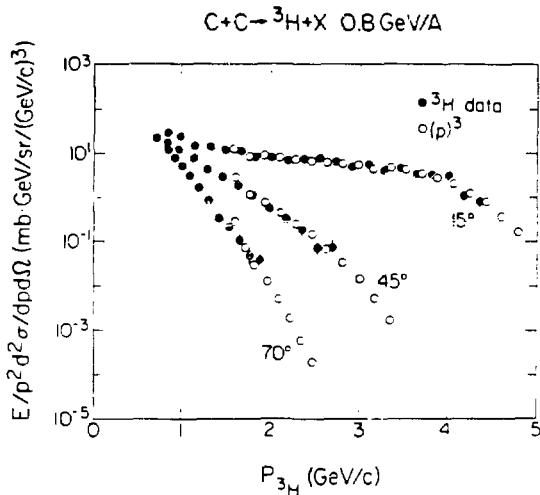


Fig. 18. Triton inclusive spectra from heavy ion collisions at 0.8 GeV/amu showing also the cube of the proton inclusive spectra at the same angles. Data from reference 9.

Figures 17,18 show how well this formula works.

While this result seems to imply a coalescence model, it would also result from local chemical equilibrium. Further information must be extracted not from the spectral shapes but from the values of C_A and their dependence on $A_{\text{projectile}}$, A_{target} , and E_{beam} . A variety of questions arise: Can we extract the source radius? What is the freeze-out density? Does the entropy change during the reaction? These questions have been addressed recently by Nagamiya^{8,9} and Stöcker¹⁹, among others.

One striking observation in inclusive spectra (not shown here) is a large excess (factors of 3-4) of neutrons compared with protons in secondary spectra below 100 MeV produced in Ne-Pb collisions. A simple explanation of this result is that neutrons and protons are depleted equally by the formation of low-isospin composites such as d, t, ^3He , ^4He , ^6Li . The depletion of protons is sufficiently extreme that the n-p ratio in the initial system is greatly amplified.

ANOMALOUS PROJECTILE FRAGMENTS

The most extensively studied part of phase space for heavy ion collisions is the projectile fragmentation region at 0° . Here the qualitative observation is that nuclear fragments are produced with velocities near the projectile velocity. The data are typically used to extract nuclear Fermi momenta. Some of the projectile fragments have very unusual neutron-proton ratios, e.g., ^{22}N or ^{44}S . Such nuclei are of interest to map out the boundaries of nuclear stability and to provide data for astrophysics calculations.

Among the projectile fragments some very remarkable objects have recently been discovered. Friedlander, et al.²⁰ exposed nuclear emulsions to ^{56}Fe at 1.8 GeV/amu. Figure 19 shows a characteristic chain of interactions. The ^{56}Fe nucleus successively fragments into particles of charge 24, 20, 11 before leaving the emulsion. As many as seven consecutive stars have been observed in such events.

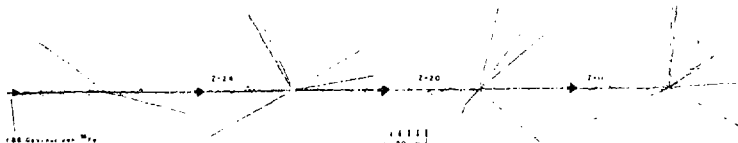


Fig. 19. A characteristic chain of interactions in emulsion following entry of a 1.88 GeV/amu ^{56}Fe (from the left). Data from reference 20.

For incident beam particles the distance before interaction can be used to extract a mean free path. Figure 20 shows such data for ^{16}O primaries and how a mean free path of 11.9 ± 0.3 cm is extracted. From similar data an empirical rule is derived:

$$\lambda_z = \Lambda_0 \lambda^{-b}$$

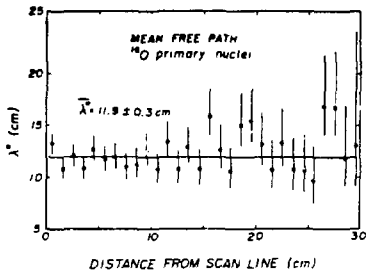


Fig. 20. Measured values of mean free path λ^* for 2.1 GeV/amu ^{16}O as a function of distance from entry into the emulsion. Data from reference 20.

If we try a similar analysis not on beam particles but on particles emerging from nuclear collisions (in the forward direction) we can use the above empirical formula to combine data with different z and accumulate good statistics. This yields the data of Figure 21, which do not follow a simple exponential absorption.

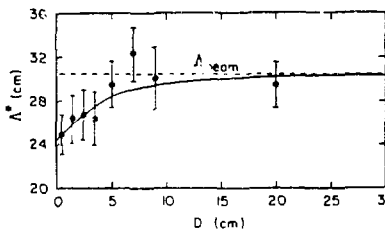


Fig. 21. Mean free path parameter Λ^* as a function of distance from the point of emission of the projectile fragments. The dashed line is the expected value. The solid line assumes a 6% admixture of "anomalons" with mean free path 2.5 cm. Data from ref. 20.

The deviation at small path lengths in Figure 21 can be explained if there is a 6% component of all fragments with a greatly enhanced interaction probability and a mean free path of 2.5 cm, less than that expected for any known nucleus, even uranium. Many speculations have focused on nuclear excitations involving quark degrees of freedom, but no theory has gained acceptance. We also await further experiments and other signatures beyond an enhanced interaction cross section.

NEXT STAGES OF EXPERIMENTATION

1. Upgraded Bevalac

In 1982 the Bevalac will have beams of all ions. This will permit equal mass collisions to be extended up to the heaviest masses. In addition, enhanced intensities of such beams as ^{56}Fe will permit counter experiments whereas only emulsion experiments have been possible in the past. Figure 22 shows the expanded capability.

In addition, we completed during 1981 two major instruments: --the HISS spectrometer, a 3 Tesla magnetic field over a 3 m diameter, 1 m gap instrumented with a flexible range of detectors.

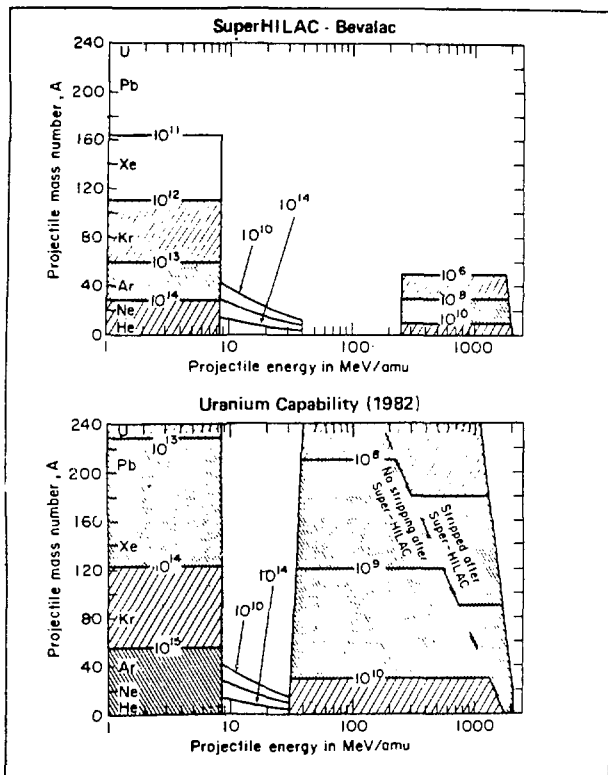


Fig. 22. Performance of the SuperHILAC-Bevalac now and after installation of a vacuum liner, presently in progress.

This will initially be concentrated on multiparticle measurements in the projectile fragmentation region, with missing mass resolution of about 1 MeV, and --the GSI/LBL Plastic Ball/Wall, with over 1000 detector telescopes covering 96% of 4π . This will permit particle identification and energy measurement over a useful range of parameters and it will make investigations of many-particle correlations much easier.

For the longer term future, LBL plans to construct a much more powerful accelerator--VENUS--which will be described below.

2. Extension to Much Higher Energies

In order to probe the transition to a quark-gluon plasma much higher energies are predicted to be necessary²¹.

Table II shows existing heavy ion accelerators and proposals for new ones. The beam momentum and range of rapidity ($y_{\text{projectile}}-y_{\text{target}}$) for each are given.

Table II

Existing and proposed accelerators for heavy ion studies, arranged in order of increasing c.m. energy. The momentum pc/A is indicated for ions with $Z/A = 1/2$, as is the rapidity range Δy between target and projectile.

	pc/A (GeV/amu)	Δy	$Z \leq 2$	$Z \leq 10$	$Z \leq 100$
Saturne	1.8	1.4	now	1981	prop
Numatron	2.6	1.7			prop
Bevalac	2.9	1.8	now	now	1982
Synchrophasotron	4.5	2.3	now	now	prop
CERN PS	13.5	3.4	now	prop	
SIS 100	15.0	3.5			prop
VENUS	25.0	4.0			prop
CERN SPS	200.0	6.1	now	prop	
CERN ISR	16.2	7.1	now	prop	
VENUS	25.0	8.0			prop

The Bevalac and the Synchrophasotron are the two presently operating heavy ion facilities. Saturne and the Numatron are expected to enter this energy range in the next several years. Saturne requires only successful operation of the CRYEBIS source. The Numatron, in Japan, is expected to be approved for construction this year.

At higher energies two major accelerators have been proposed: SIS 100 at GSI, Darmstadt, and VENUS at LBL. VENUS comprises both fixed target and colliding beam facilities, the latter being about 60% higher in energy than the ISR. In addition to these, the CERN

facilities that have already accelerated alpha particles are obvious candidates for extension into the $Z \leq 10$ region, which could be done with investment of about \$10 M.

Figure 23 is a graphic representation of Table II, constructed so as to explore the capabilities of each accelerator in terms of parton concepts of the hadronic interaction. The target and projectile rapidities are shown as a function of γ_{cm} . It is assumed that target and projectile fragments (i.e., fragments of the nucleons) will occur in a region within ± 2 units of rapidity of the target and projectile rapidities, respectively.

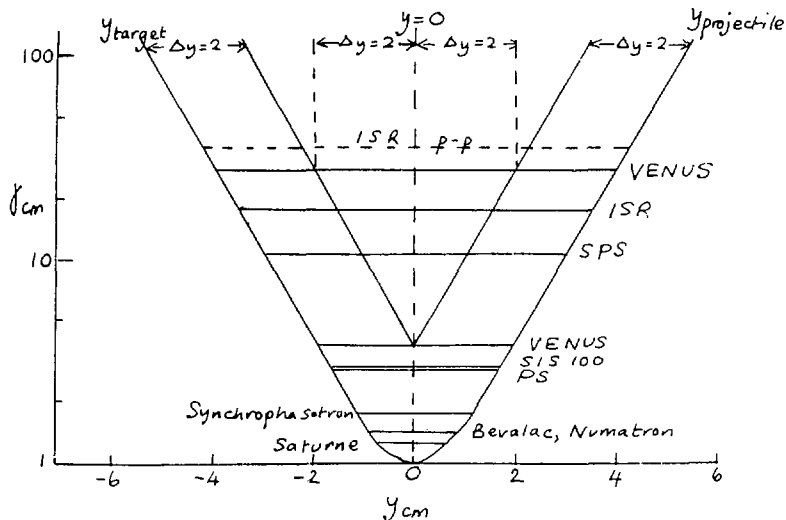


Fig. 23. The center of mass Y plotted versus c.m. rapidity for target and projectile. Lines at $y_{\text{target}} + 2$ and $y_{\text{projectile}} - 2$ are intended to suggest the range of short-range rapidity correlations. A clearly separated central rapidity region exists at ISR and VENUS energies.

We thus see that at the four low energy accelerators the partons from projectile and target may be expected to overlap. New states involving all the quarks in both target and projectile might be possible. At the highest energy accelerators, the projectile and target fragmentation regions are well separated and there is a large central region of created particles as well.

The energy of the ISR was well chosen to elucidate the rapidity structure of the p-p collision. It falls by a factor of two for ions ($Z/A = 1/2$). The VENUS design energy was increased above that of the ISR to compensate for this factor. Note also that the VENUS

fixed target capability has a reasonably well-separated target and projectile fragmentation region.

The high energy accelerators would permit study of the central region of created quarks and gluons and of high density states involving the quarks of either target or projectile but not both.

In passing, note the values of γ . With $\gamma_{cm} = 25$, two colliding uranium nuclei would both be contracted to less than the thickness of a proton, providing the ultimate possibility of coherent multi-quark interactions. With $\gamma_{lab} = 25$ (fixed target capability of a collider with $\gamma_{cm} = 25$) the projectile uranium nucleus, viewed in the laboratory frame, is contracted to the thickness of a proton. In this case also, interesting coherent effects must occur and the entire collision must be considered at a parton level.

3. ISR Experiments

Recent α - α and p - α experiments at the ISR give our first look beyond p - p collisions. Some preliminary results are available²², while much further data are being analyzed.

Starting from the most predictable quantity, R418 reports a preliminary uncorrected value of 255 ± 20 mb for the total inelastic cross section. Since their detector gave an uncorrected value for the p - p total inelastic cross section that was about 7% low, the α - α result should presumably be increased by about 7%, i.e., to 290 ± 20 mb. This may be compared with a Bevalac measurement of 276 ± 15 mb and a Dubna measurement of 304 ± 20 mb. Clearly there is no surprise.

R418 also report a measurement of the rapidity distribution of secondary particles. This is shown in Figure 24. The positive and negative distributions agree quite well near $y_{cm} = 0$ indicating a

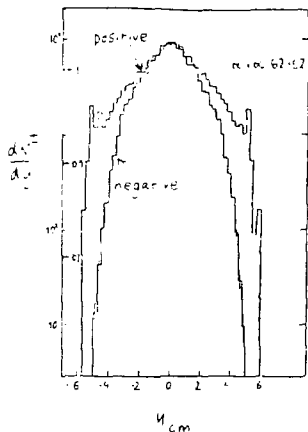


Fig. 24. Rapidity distributions for positive and negative particles produced in α - α collisions at 15.5 GeV/amu c.m. Preliminary data from R 418, ref. 22.

clear separation of the central region from the target fragmentation region. The central value $(dn/dy)_{y=0}$ is difficult to compare with the p-p value since the p-p data were taken at twice the energy. However, after correcting for the known energy dependence in p-p collisions it is found that

$$\left(\frac{dn}{dy}\right)_{aa,y=0} / \left(\frac{dn}{dy}\right)_{pp,y=0} = 1.8 \pm 0.1$$

This value is consistent with the constituent quark model prediction of Bialas and Czyz²³, in which the central region production results from the breaking of colored strings.

Another early result is on the p_T dependence of π^0 production, which demonstrates the existence of coherent effects. Figure 25 shows the ratio of the cross section to that for p-p

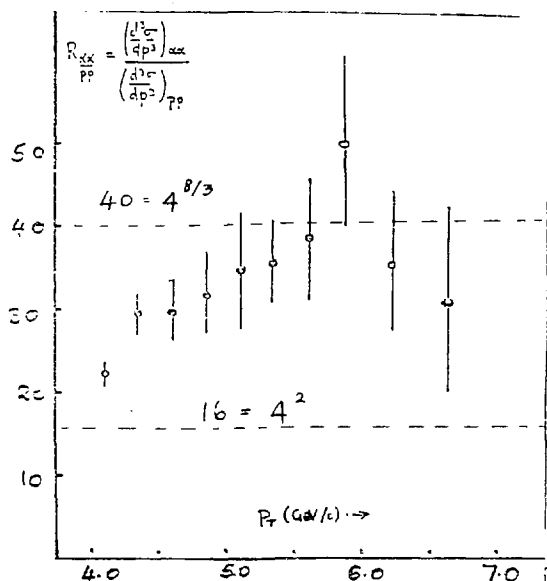


Fig. 25. Ratio between π^0 production in AA collisions and p-p collisions at 15.5 GeV/amu c.m. Preliminary data from R 108, ref. 22.

collisions. The yield is substantially greater than the value of $A^2 = 16$, which would be the most optimistically large value in the absence of coherent effects. It is remarkable that this effect, previously observed in p-A collisions by Cronin, et al.²⁴ should show up in such a small system.

It will be interesting to see the other results when they become available. It would be even more interesting to extend the value of A. As I indicated earlier, this could be done at least up to $Z \approx 10$ by constructing a new linac injector at a cost of about

\$10 M. Some of us are presently exploring the possibility of an interregional consortium to extend the life of the ISR for a program of light ion research after its scheduled closure for particle physics at the end of 1983.

4. Very Heavy Beams and Very High Energies

For a full program a dedicated accelerator is necessary, with beams of the heaviest ions and comprehensive facilities for both fixed target and colliding beam research. Figure 26 shows the layout for the VENUS facility at LBL²⁵, which is injected by beams from the existing SuperHILAC. It could be operating by the end of 1988 but has not yet been approved for construction.

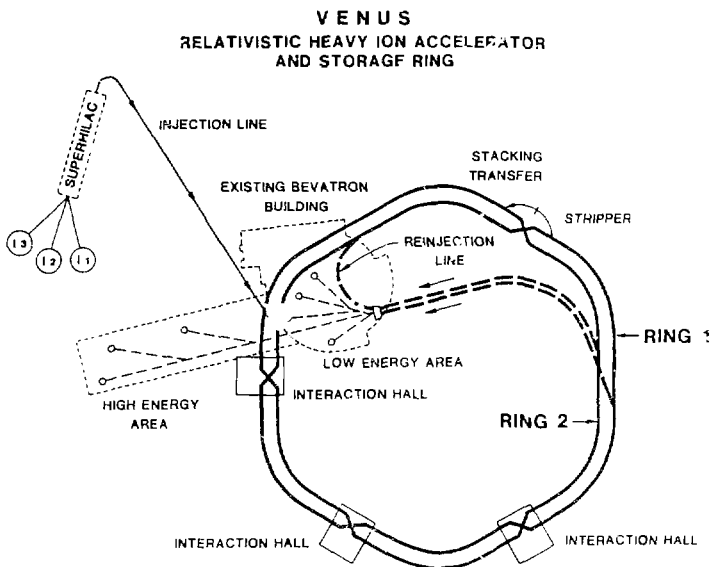


Fig. 26. One of the proposed layouts for the VENUS accelerator at LBL. The facility will include fixed target and colliding beam capabilities at 25 GeV/amu for $Z/A = 1/2$ (50 GeV protons, 20 GeV/amu uranium).

What could one expect in a U-U collision at these energies?

1) If the coherent enhancement of high p_T yields continues, we may expect $1-2 \cdot 10^6$ times the yield at high p_T compared with p-p collisions.

2) If we use Landau theory to scale from p-p to A-A collisions, we obtain the results shown in Figure 27. The left-hand scale shows the multiplicity observed in p-p collisions, while the right-hand scale shows the projected multiplicities for U-U collisions. The latter are enormous. Note in particular the large yields of kaons, which might permit production of multistrange objects.

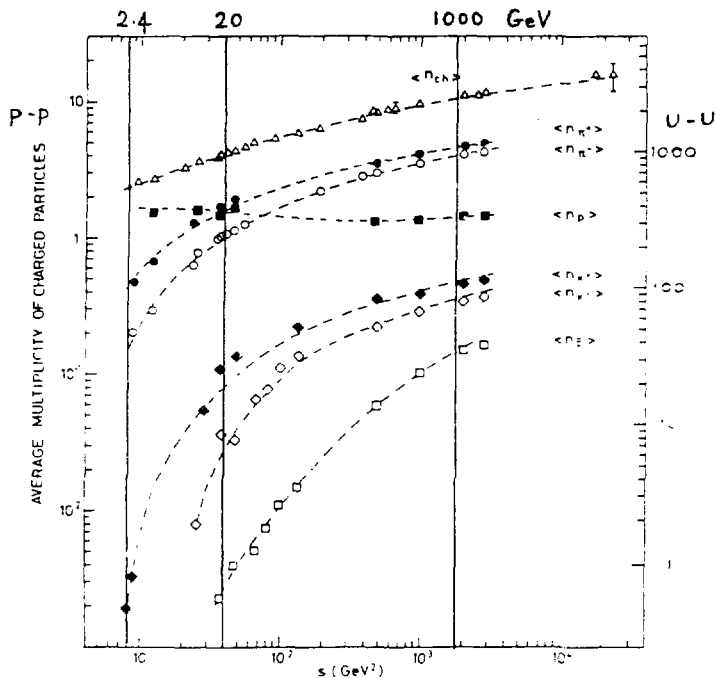


Fig. 27. Measured charged particle multiplicity in p-p collisions and an extrapolation to U-U collisions at the same energy per nucleon.

3) Finally, an important reason to go to large A is to create a system in which equilibrium has a chance to become established. In this context, Kajantie and Miettinen²⁶ have calculated the transition from quark-gluon plasma to hadron gas for a U U collision. They find that there would be 50,000 gluon-gluon collisions and 4000 quark-gluon collisions in the cooling-down stage, surely enough to make statistical considerations not only valid but inescapable.

ACKNOWLEDGMENTS

I am grateful to my colleagues, especially Andres Sandoval and Rainer Renfordt, in the LBL/GSI streamer chamber collaboration for figures and unpublished data and to Shoji Nagamiya for providing figures and unpublished data from the LBL/INS collaboration.

This work was supported by the Director, Office of Energy Research, Division of Nuclear Physics of the Office of High Energy and Nuclear Physics of the U.S. Department of Energy under Contract W-7405-ENG-48.

REFERENCES

1. 1st Workshop on Ultrarelativistic Nuclear Collisions, Berkeley, May 21-24, 1979, LBL-8947
2. International Conference on Extreme States in Nuclear Systems, Dresden, February 4-9, 1980; Proceedings ed. H. Prade, S. Tesch, ZfK Rossendorf, ZfK-430 (1980)
3. Hakone Seminar (Japan-U.S. Joint Seminar) on High-Energy Nuclear Interactions and Properties of Dense Nuclear Matter, July, 1980; Proceedings eds. K. Nakai, A.S. Goldhaber, Hayashi-Kobo, Tokyo (1980)
4. Workshop on Future Relativistic Heavy Ion Experiments, GSI, Darmstadt, October 7-10, 1980; Proceedings eds. R. Bock, R. Stock, GSI 81-6 (1981)
5. 5th High Energy Heavy Ion Study, Berkeley, May 18-22, 1981; Proceedings ed. L.S. Schroeder, to be published early 1982
6. K.K. Gudima, V.D. Toneev, Dubna preprint E2-12624 (1979)
7. V.M. Galitzky, I.N. Mishustin, ref. 2, vol. 2, 131
8. S. Nagamiya, ref. 5 and LBL-12950 (1981)
9. S. Nagamiya, et al., LBL-12123 (1981)
10. M. Gyulassy, International Conference on Nuclear Physics, Berkeley, August 24-30, 1980; Proceedings eds. R.M. Diamond, J.O. Rasmussen, North Holland Publishing Company, Amsterdam, p. 395c.
11. Y. Yariv, Z. Frankel, Phys. Rev. C20 (1979) 2227
12. A. Sandoval, et al., Phys. Rev. Lett. 45 (1980) 874
13. R. Hagedorn, ref. 4, p. 236
14. Preliminary data, LBL/GSI Streamer Chamber Collaboration
15. M. Gyulassy, S.K. Kaufman, L.W. Wilson, Phys. Rev. C20 (1979) 2267 and references therein
16. Private communication, M. Gyulassy
17. J.W. Harris, et al., Phys. Rev. Lett. 47 (1981) 229

18. A. Shor, et al., contributed paper, ref. 5
19. Horst Stöcker, LBL-12302 (1981)
20. E.M. Friedlander, et al., Phys. Rev. Lett. 45 (1980) 1084; see also H.H. Heckman, LBL-12656 (1981)
21. L. McLerran, invited paper at this meeting; R. Anishetty, P. Koehler and L. McLerran, Phys. Rev. D22 (1980) 2793
22. M.G. Albrow and M. Jacob, eds., Discussion Meetings between Experimentalists and Theorists on ISR and Collider Physics, Ser. 2, Nos. 2,3, CERN EP and TH preprints (1981); M. Faessler and M. Jacob, invited papers, ref. 5
23. A. Bialas, W. Czyz and L. Lesniak, Report INP-1141/PH and TPJU-10/81, Cracow (1981)
24. J.W. Cronin, et al., Phys. Rev. D11 (1975) 3105
25. The VENUS Project, LBL PUB-5025 (1979)
26. K. Kajantie and H.I. Miettinen, University of Helsinki Research Institute for Theoretical Physics, Preprint HU-TFDT-81-7 (1981)